Current Distribution in a Reusable Junction for W7X Coil Tests

T. Schild, J. Germain, J.B. Berton, B. Dupont, and A. Forgeas

***Abstract*--In the frame of the W7X stellerator project, CEA has to perform the acceptance tests of the 70 coils of the magnet system. A new test facility has been built at Saclay for that purpose. As the coils are delivered to CEA with bare end, it has been necessary to develop a junction that can be easily applied on a CIC conductor and that can be easily dismantled and reusable due to the large number of coils to be tested. As inhomogeneous current distribution within the conductor could lead to unexpected low quench current (i.e. ramp rate limitation), an experiment has been developed in order to estimate that distribution at the outlet of the junction. The experimental set-up is made of 16 pick-up coils measuring the current within the 16 sub-stages of the CIC (Cable-In-Conduit). This paper will present our experimental results and the conclusion of our analysis.**

***Index Terms*— Current distribution, Cable In Conduit, Junction, Pick-up coil.**

I. Introduction

The junction principle is a classical contact pressure over an indium foil (contact pressure junctions are used at the SULTAN Test facility, CRPP, Switzerland, at TOSKA Test facility, FzK, Karlsruhe).

In our case, the contact pressure has to be minimized to prevent damages of the junction after several tests. That is why some tests measuring the resistance as a function of the contact pressure have been performed. Part II presents these preliminary results. They have shown a possible current unbalance beyond the junction. Such inhomogeneous currents could lead to low quench current that is why they have often been investigated for various kinds of superconductor [1-3].

Then, an experimental set-up has been developed in order to measure that distribution within our junction. This distribution has been measured versus the contact pressure, the ramp rate and the maximum applied current. It was possible to estimate the resistance distribution at the contact surface (Part IV).

II. Overview of the Junction

A. Design

The junction design is based on the W7X demonstrator coil (the so-called 'DEMO' coil) junction developed at FzK, Karlsruhe. Fig. 1 presents the assembling principle. From the bottom to the top, the junction is composed of:

- A copper plate where 16 grooves have been machined. In each grooves, the two first stages of the conductor (3x4) are soldered.
- The Inox casing of the junction. It is linked to the copper plate by explosive bonding. The conductor input is located on the left side , and the helium output on the right one.
- A rectangular metallic seal insert in the groove of the Inox casing.
- An Inox plate to guide the helium flux along the cooper plate.
- An Inox cover to close the junction through the metallic seal.

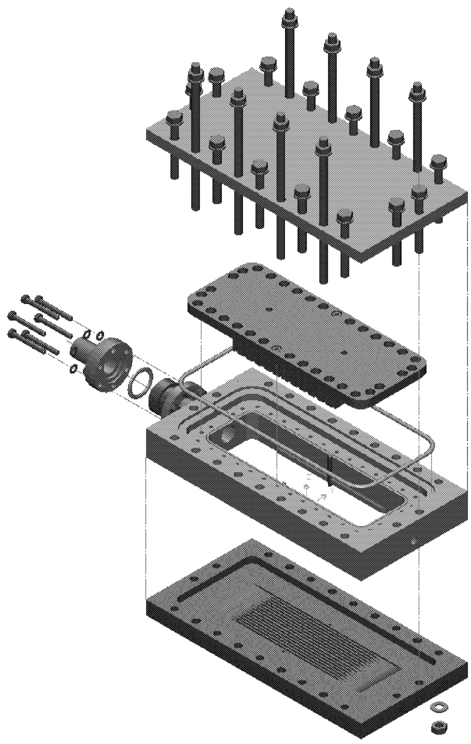

Fig. 1 Junction design, principle of assembly

To make a connection, one junction box is assembled at each end of the conductor to link. Then the two boxes, in between which an indium foil (0.1 mm thick) is placed, are pressed together. The pressure is applied through 8 screws M10 for this prototype (M8 on serial junctions).

Manuscript received September 24, 2001.

Th. Schild (corresponding author, telephone: 33 1 69 08 37 75, e-mail: thierry.schild@cea.fr), J. Germain, J.B. Berton, B. Dupont, and A. Forgeas are with CEA Saclay (Dapnia), F-91191 Gif-sur-Yvette, France.

B. *First experimental set-up*

In order to validate the design, and also to define the working pressure, cryogenic tests have been performed in liquid helium bath for different contact pressure values, without background magnetic field. The junction is equipped with 5 voltage taps as described in Fig. 2.

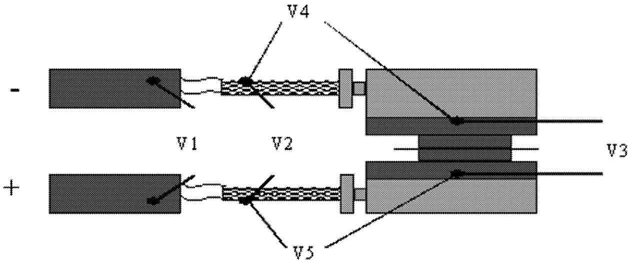

Fig. 2 Experimental set-up for resistance measurements

The measurements results are presented in Fig. 3.

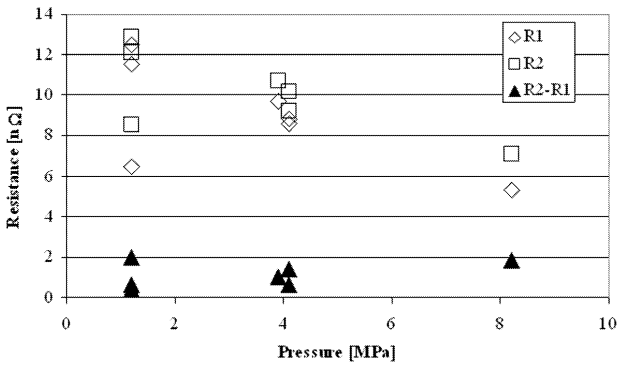

Fig. 3 Resistance measurements results.

C. *Analysis*

A decreasing of the total resistance, R_2, as a function of the increased contact pressure is observed, as expected. It has also to be noted that all measured values are below our design value of 20nΩ. Moreover, it can be seen that the total resistance is dominated by the contact resistance, R_1 (i.e. R_1 is nearly equal to R_2). However, for rather high pressure values, i.e. at 8 MPa, it has been observed that a resistive voltage on voltage taps V_4 and V_5 (then R_1 is lower than R_2).

A possible origin for such a voltage drop could be a current redistribution within the conductor beyond the junction. As recalled in the introduction, such non-uniformity could lead to unexpected low quench current for the coil. Then in order to check our assumption, an experimental set-up using pick-up coils has been designed to measure the current distribution inside the connection. In other words, our goal is to measure the current in each strands groups (see Part II.A).

III. Current distribution measurements

A. *Principle*

The principle is to apply a pick-up coils network above the connection copper plate. There is one pick-up coil above each of the 16 grooves. Fig. 4 shows a sketch of the pick-up coils set-up. During a current ramping, the voltage induced in each pick-up coil is proportional to the current variation in each strands group. Then, from the pick-up coils voltages, it is possible to calculate the current in each group. For that purpose, it is necessary to calculate the induction on each pick-up coil due to the current flowing in each strands group.

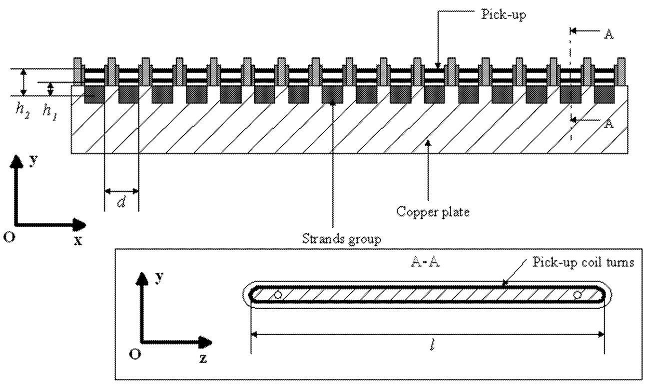

Fig. 4 Pick-up coils set-up above the copper plate and pick-coil cross-section.

B. *Calculation*

Some assumptions have been done in order to simplify calculation work:

①As strands are in superconducting state, the current within a strand group linearly increases according to direction **z** (see Figure 4). It means, if *L* (60 mm) is the length on which strands are soldered that

$$I(z,t) = I_{Total}(t)\, z/L\,. \tag{1}$$

②Due to the strands twisting, current is uniform inside a group.

③A strands group has a circular cross-section.

④Due to assumption ① and because the resistance of the contact surface is assumed to be independent from x, the current flowing from junction (+) to junction (-) can be modeled as 16 current sheets in the direction **y** with uniform current density. After computation, it has been found that these currents lead to negligible inductions on pick-up coils compared to the effect of currents flowing within grooves in direction **z**.

⑤Currents in group *i* of junction (+) and in the group *i* of junction (-) are identical, due to the symmetry of junctions.

Let us call I_i the current within the strands group *i*. Let us call $B_{ij}^{(+)}$ the average induction due to group strands *i* from junction (+) on the pick-up coil *j*. Let us call $B_{ij}^{(-)}$the average induction due to group strands *i* from junction (-) on the pick-up coil *j*.

It can be shown that

$$B_{ij}^{\pm} = \pm\frac{5m_0 I_j}{4pLS}\sum_{n=-10}^{9}\iint_{y,z}\frac{y}{d_{ij}^2+y^2}\left(\begin{array}{c}\sqrt{y^2+d_{ij}^2+z^2}-\\ \dfrac{y^2+d_{ij}^2+z^2-zL}{\sqrt{y^2+d_{ij}^2+(z-L)^2}}\end{array}\right)dydz\,, \tag{2}$$

with $d_{ij} = d\left|i-j\right|$, where *d* is the distance between pick-up coils *i* and strand group *i*+1 (see Fig. 4), and S is the pick-up section. *z* is integrated between *L-l* and *l*, *l* is the length of the pick-up (see Fig. 4). y is integrated respectively between h_1 and h_2 for junction (+), h_1+D and h_2+D for junction (-). D is the distance between grooves of junction (+) and junction (-).

It is then possible to build the square matrix 16x16 $\underline{\underline{L}}$ so that :

$$\underline{\Phi} = \underline{\underline{L}} \cdot \underline{\dot{I}} \ . \qquad (3)$$

Thanks to Eq. (3) it is possible to calculate each strands group current I_i knowing the voltage drop V_i during the current ramping up as :

$$\underline{V} = -\frac{d\underline{\Phi}}{dt} \ . \qquad (4)$$

C. Experimental set-up

All experiments are performed in helium bath at 4.2 K without background field. The sample is energized by a power supply of 10 kA, 5V. The data acquisition system is equipped with 32 instrumentation amplifiers (x800). The maximum sampling rate used is 5 kHz.

D. Results

All runs are summed up in Table I. R_i is the resistance calculated from voltage drop V_i (see Fig. 2). For each run, the current has been ramping up between 500 A/s and 2000 A/s.

TABLE I
EXPERIMENTAL RESULTS

Run ID	Torque daN.m	R_1 nΩ	R_2 nΩ	R_3 nΩ	R_4 nΩ
1	0.5	33.8			
2	1.0	23.8	26.2	1.44	0.88
3	2.0	13.9	14.8	0.42	0.64
4	0.3	12.7	14.2	0.73	0.72
5	0.5	3.7	5.7	0.87	1.08
6	1.0	3.7	5.4	0.73	0.92
7	1.5	3.7	5.2	0.68	0.93
8	0.5	55.3	57.6	0.79	1.57
9	0.5	450			
10	0.5	140	143.3	1.29	3.03

First, it can be seen that since run 8, the junction resistance, R_1, is higher than in previous experiments (see Fig. 3). A clear degradation of the junction has appeared.

Secondly, as in the previous experiments, the voltage drop V_3 and V_4 are quite low compared to the others. The main resistance is still due to the pressure contact.

Thirdly, the presented calculations can be checked by summing all currents and compared them to the measured power supply current. Fig. 5 shows that the agreement between calculation and measurements is good. The maximum error found for all runs is below 12%. Fig. 6 gives the results of the current calculation within each strands group for the same run.

E. Conclusion

The currents calculated with pick-up coils measurements seem in good agreement with direct measurements (total current), it is then possible to analyze the current distribution within the junction.

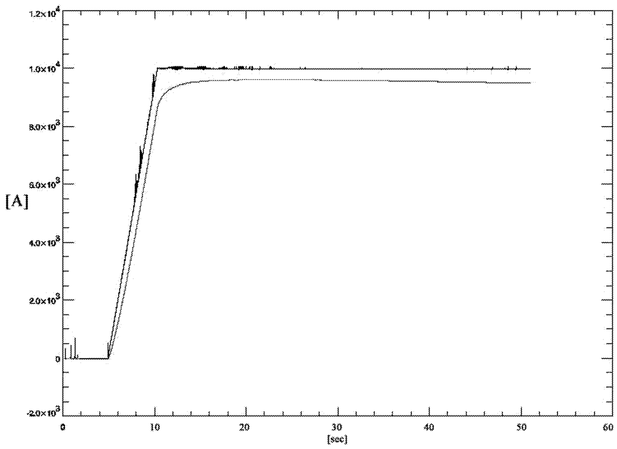

Fig. 5 Comparison between measured (upper curve) and calculated (lower curve) current for a ramping rate of 2000 A/s.

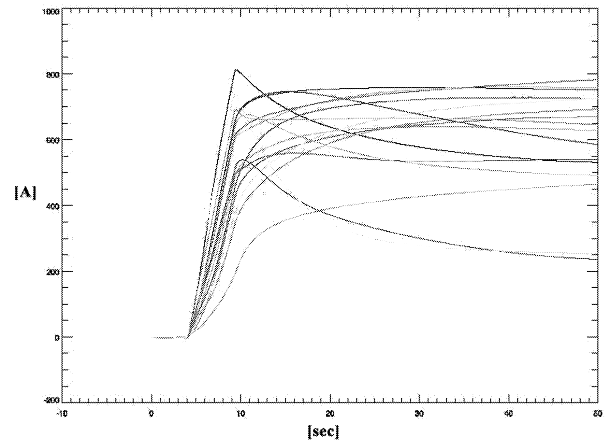

Fig. 6 Current distribution within the 16 strands groups as a function of time.

IV. ANALYSIS

Our main goal is to measure the current distribution in steady state conditions. In that case, the distribution is driven by the resistance distribution between the two copper plates as the other resistances (R_3 and R_4) are considered as negligible (see Table I). According to assumption ⑤, there is no current transfer between strands group, it is therefore possible to model the total junction as 16 isolated parallel resistance r_i. r_i is then the resistance between strands group i of the junction (-) and strands group i of the junction (+). It can be easily shown that

$$r_i = R_1 \, I_{Total} / I_i \ . \qquad (5)$$

A. Effect of the ramping rate

According to experimental results as a function of the ramping rate and the maximum current applied, the calculation of the resistance distribution for a given torque is independent of the ramping rate (computations are carried out when steady state conditions are reached), and of the maximum current applied.

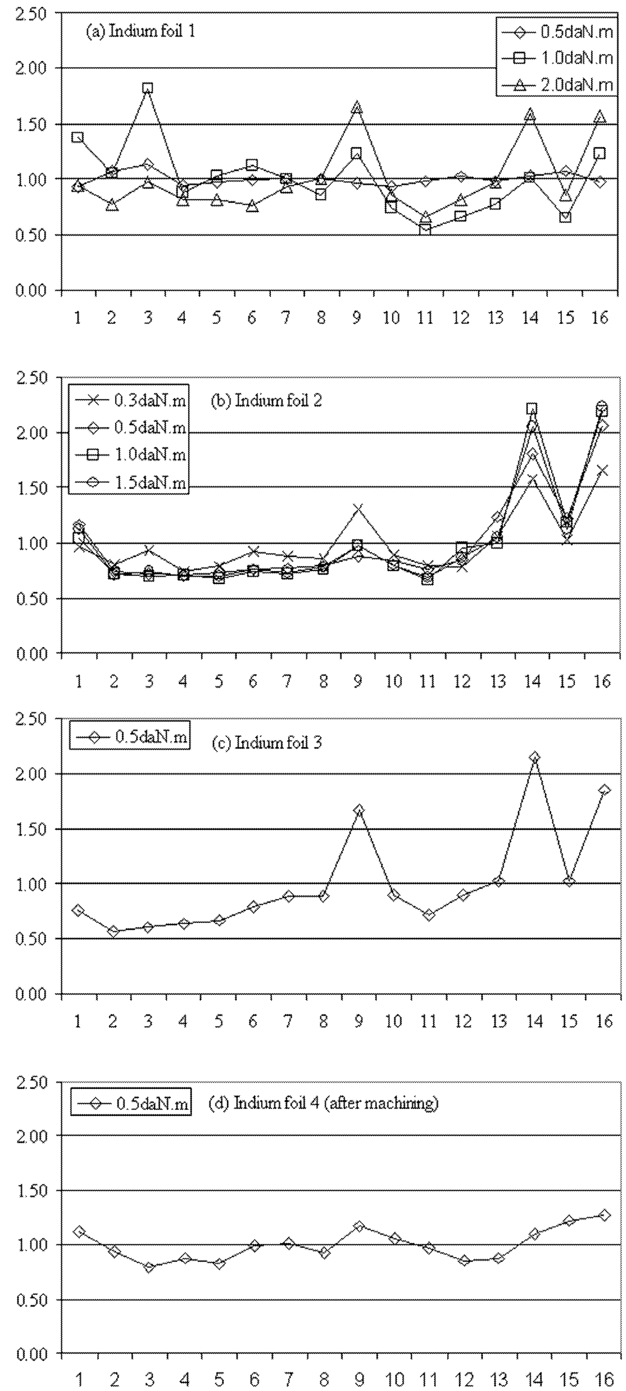

Fig. 7 Resistance distribution normalized to $R_I/16$ as a function of the strands group and the torque for indium 1 (a) , 2 (b), 3 (c) and 4 (d).

B. Effect of the torque

Four indium foils have been used with different pressures. Fig. 7 presents distribution resistance measured as a function of the torque and the strands group. According to Fig. 7.a, it seems that the resistance distribution is very sensitive to the torque as for 0.5daN.m the distribution is quite homogenous and, for 2.0daN.m, it is inhomogeneous.

But, regarding Fig. 7.b, it appears that the distribution is quite the same from 0.3daN.m to 1.5daN.m.

In fact, it can be noted that after the run 2 (see Table I), three peaks (for strands group 9, 14 and 16) appear on every tests (see Fig. 7.b and Fig. 7.c). Meanwhile, the contact resistance is degraded (especially in run 8 and run 9).

As a deformation of contact surfaces has been suspected, they have been machined in order to find back a good surface state. Fig. 7.d shows that after machining, a good resistance homogeneity is found, as in run 1. It shows that the contact surface were mechanically deformed during run 2 or 3.

The high resistance measured for run 10 is certainly due to a contact resistance oxidation because contact surfaces were not gold coated as for previous experiments.

V. Conclusion

The method of measuring the current distribution using pick-up has shown a good reproducibility and a good accuracy. The analysis of our results versus the pressure applied on the junction have shown that the current distribution is not very influenced by the contact pressure up to a torque of 2 daN.m per screw. Moreover, the current distribution is quite homogenous regarding all tests. It has to be noted that the current unbalance is lower than the unbalanced expected for ITER TF Model coil [4], and this coil has been successfully tested at full current.

In future, it is foreseen to adapt the model developed by ITER for TFMC in order to estimate the current distribution at the peak field of the coil [5].

A mechanical irreversible deformation of the contact surface has been pointed out during tests. This deformation demonstrates that the contact pressure has to be applied with a great care in order to avoid a local deformation of the surface. Nevertheless, this deformation could be recovered by surface machining.

VI. Acknowledgment

The authors thank all the W7X team at CEA.

The authors would like also to thank the Development and Measurement Group from the cryogenic and magnetic service for its help during testing period, especially MM. Kulbicki , Paladji and Carré.

The authors have also appreciated the discussions with F.P. Juster for modeling the current distribution.

VII. References

[1] N. Mitchell, *Modelling of non uniform current diffusion coupled with thermohydraulic effects in superconducting cables*, Cryogenics 2000, Vol. 40, pp. 637-653.

[2] A.P. Verweij, L. Buchsbaum, *Experimental results of current distribution in Rutherford- type LHC cables*, Cryogenics 2000, Vol. 40, pp. 663-670.

[3] T. Hamajima, A.K.M. Alamgir, N. Harada, M. Tsuda, M. Ono, H. Takano, Analysis of current distribution in a large superconductor, Cryogenics 2000, Vol. 40, pp. 729-736.

[4] T. Schild, D. Ciazynski, Court S, *Effect of actual cabling pattern on the critical current of a multistage CIC*, Advances in cryogenic engineering – Materials, Vol. 46B, pp. 1051-1058.

[5] D. Ciazynski, *Conductor analysis tools*, Internal note, CEA/DRFC/STEP.